Available online at www.sciencedirect.com
ScienceDirect
Journal of Power Sources 162 (2006) 151–159
JOURNAL OF POWER SOURCES
www.elsevier.com/locate/jpowsour

Electrocatalysis of oxidation of hydrogen on platinum ordered intermetallic phases: Kinetic and mechanistic studies

A.F. Innocente, A.C.D. Ângelo *

Laboratório de Eletrocatálise, Departamento de Química, Faculdade de Ciências, UNESP, PO Box 473, Bauru 17033-360, SP, Brazil

Received 17 May 2006; received in revised form 19 June 2006; accepted 21 June 2006
Available online 22 August 2006

Abstract

An experimentally based kinetic and mechanistic study of the hydrogen oxidation reaction (HOR) on platinum and platinum ordered intermetallic materials in acid medium is presented. RDE kinetic data were re-evaluated and complemented by Tafel plots obtained from chronoamperometric measurements. Among the materials evaluated, PtSb and PtSn exhibited markedly improved kinetic current densities and exchange current densities, compared to Pt in the same experimental conditions. It is proposed that the intermetallic phase enhanced the adsorptive characteristic of the surface sites and, as a consequence, improved the kinetics of the adsorption steps (Tafel or Heyrovsky) of the mechanism involved.

Keywords: Platinum; Ordered intermetallic phase; Hydrogen oxidation; Kinetic; Adsorption; Electronic effect

1. Introduction

The mechanism of the hydrogen oxidation reaction (HOR) that occurs at the anode of a proton exchange membrane fuel cell (PEMFC) is well known and widely discussed in the literature [1,2]. HOR involves the transfer of two electrons from the H_2 molecule and may follow different pathways, the most plausible in acid medium being the Tafel–Volmer and Heyrovsky–Volmer mechanisms (ibid.).

Seminal work by Gasteiger et al. [3–5] has shown that this reaction runs smoothly and quickly on platinum-based catalysts [6] and that, at higher current densities, it is controlled by diffusion, i.e. by mass transport [1]. Although the reaction may be extremely fast on a platinum surface, a serious problem arises when the system is fed with impure hydrogen generated by the catalytic reform of substances derived from the biomass (natural gas, methanol, ethanol etc.). In this case, small amounts of carbon monoxide are co-produced and this compound is adsorbed strongly at active surface sites on Pt, irreversibly contaminating the electrocatalyst and so diminishing the catalytic activity of the electrode [7]. Another disadvantage of platinum as a catalyst for the HOR is its high price and the possible depletion of mineral reserves if fuel cells were to become more widely used [8].

In light of these remarks, catalytic electrodes will have to be developed in materials other than platinum, if fuel cells are to become a practical alternative way of producing energy. The main features that would be required of a good electrocatalyst for HOR are low susceptibility to carbon monoxide poisoning (when the source of the hydrogen fuel is catalyzed reform of organic matter) and a low price, to allow fuel cells to compete with the energy-transforming systems in general use nowadays.

A convenient strategy that has been used repeatedly by many research-workers to develop new electrocatalysts and to investigate the reactions occurring in fuel cells is to modify a platinum electrode by depositing atoms of elements such as Sn, Ru, Bi, Mo, Cu, etc. on its surface. This approach has given excellent results from the start [9–20]. While some details of the mechanism remain unclear, the action of the deposited atoms is generally attributed to one or more of the following: a modification of the electron density at the surface sites [12,17,20–22] that favors desorption of CO; the availability of oxygenated species on the surface, favoring oxidation of the non-reactive CO intermediate [23–25]; or a 'third-body' effect that makes it less likely that the poisonous intermediate will be adsorbed in a stable configuration on the electrode surface [23,26]. Notwithstanding the notable scientific achievements of this research strategy, there are still a number of unresolved questions regarding the

* Corresponding author. Tel.: +55 14 3103 6093; fax: +55 14 3103 6093.
E-mail address: acangelo@fc.unesp.br (A.C.D. Ângelo).

0378-7753/$ – see front matter © 2006 Published by Elsevier B.V.
doi:10.1016/j.jpowsour.2006.06.057

influence of the deposited atoms on the course of the electrocatalyzed reactions, and about the applicability of these discoveries to real systems, in view of the technical limits imposed by the physical–chemical instability of the modified surfaces.

At this stage of the research in this area, a new methodology is called for that is sufficiently reliable to be closer for application in real electrochemical systems. In this context, preliminary work on ordered intermetallic phases shows great promise for future development. These materials offer the possibility of controlling the electron density pattern and the disposition of active sites over the surface, by varying the elements present in the intermetallic phase and their stoichiometry, so as to modulate the adsorption of H_2 at the electrocatalytic surface. Other advantages of these metal phases *vis-à-vis* potential real applications are their great physical–chemical stability and their lower cost of production, resulting from the reduced proportion of platinum. Regarding the need to use H_2 contaminated with CO (produced in the catalytic reform of hydrocarbon fuels), the catalytic sites of these new materials could furnish oxygenated species at lower anode potentials than required on the surface of Pt, thus favoring the oxidation of adsorbed CO and freeing blocked active sites for the oxidation of H_2, or the distance between neighboring surface adsorption sites could even be changed, thus inhibiting the irreversible adsorption of CO. In the last few years, intermetallic phases have been adopted as a major line of research [27,28], but until now no concrete information has been published on the influence of the electron density pattern, disposition or element content of surface sites on electrocatalytic reactions.

One reliable way of evaluating intermetallic phases with respect to electrocatalysis of the HOR is to investigate the kinetics of the reaction, which can be done conveniently with a rotating disk electrode (RDE) technique. Since the HOR is an extremely rapid reaction, the diffusion of gas dissolved in the electrolyte towards the surface of the electrode has to be augmented, to prevent the supply of electroactive element to that surface from running out. For this reason, the RDE technique is frequently used to study the oxidation of H_2, as it allows the mass transport in the electrolyte to be enhanced in a highly reproducible way [29], so that the steady-state conditions in a real fuel cell can be simulated [3]. Gasteiger et al. [3] collected data on the electrocatalysis of the HOR on polycrystalline platinum, using RDEs at various speeds of rotation (100–3600 rpm) and potentials of 0–0.3 V, in a solution of 0.5 M H_2SO_4 saturated with H_2 at room temperature. Their work confirmed that the HOR on platinum is a very fast reaction, with a minimum kinetic current density (i_k) of 60 mA cm^{-2}. In the same study, the HOR was also tested on the surface of PtRu, where i_k was found to be 30 mA cm^{-2}. However, no analysis was made of the nature of the electrocatalytic action of this material. Similar results were obtained by Chialvo et al. [2], who used a rotating disk electrode to study the effects of hydrogen diffusion on the kinetics of the HOR at the surface of polycrystalline platinum. In these experiments, the RDE rotated at 900–8100 rpm, at potentials between −0.05 and 0.4 V, in a 0.5 M H_2SO_4 solution saturated with H_2, at 30 °C, and the value found for i_k was 240 mA cm^{-2}, verifying once again the high reaction rate of the HOR. The results cited above demonstrate unequivocally how effective the RDE technique can be in the study of the kinetics of the HOR on electrocatalytic materials.

In spite of the suitability of the RDE technique for kinetic studies of HOR, it is somewhat uncertain and imprecise in measuring the corresponding kinetic data. Thus, it is generally considered necessary to confirm the RDE results by another steady-state technique (polarization curves—Tafel plots) that also provides kinetic parameters, besides mechanistic information.

From this short review of the current situation, it is evident that more complete, detailed and well-planned experiments must be done, in order to characterize the oxidation of hydrogen by electrocatalysis on Pt-based electrode materials. No less importantly, such a study should furnish reliable scientific information on which to base a theory of the mechanism of electrocatalysis of the HOR. Hence, in this article we present a study of the kinetics of the oxidation of H_2 on the surface of anodes made of the ordered intermetallic phases PtMn, PtPb, PtSb and PtSn, carried out so as to gain fundamental information on the electrocatalysis of this reaction.

2. Experimental

The intermetallic phases PtMn, PtPb, PtSb and PtSn were prepared from the respective pure metals, which were weighed in 1:1 stoichiometric proportions and melted together in an electric-arc furnace, in an argon atmosphere. The melting conditions were selected from the corresponding phase diagrams [30]. The metals were obtained in the following forms: platinum sheet (Alfa Aeasar, 99.9% pure), powdered manganese (Alfa Aeasar, 99.95%) and granulated lead (Baker, 99.9%), antimony (Aldrich, 99.9999%) and tin (Berzog, 99.9%). Each melt was homogenized and transferred to a thermal induction furnace (Inductoheat) with a prefixed thermal gradient, in which the direction and rate of solidification could be controlled. This furnace was held for 24 h at the temperature at which the desired phase was stable (taken from the appropriate phase diagram), with an atmosphere of argon, after which the material was quenched rapidly, so as to maintain this phase unchanged. The cylindrical ingot thus produced was sectioned with a diamond-impregnated rotary saw into disk-shaped test-pieces, which were used both for the characterization of each material and for the construction of the rotating-disc electrodes (RDEs) for the electrochemical experiments.

The materials were characterized by X-ray diffraction (XRD), using a Rigaku RINT-Ultima diffractometer and a Cu cathode as source of radiation ($\lambda = 1.5406$ Å). Moreover, intermetallic samples were submitted to analysis by X-ray photoelectron spectroscopy (XPS), using radiation from a synchrotron at Laboratorio Nacional de Luz Sincroton (LNLS) Campinas, SP, Brazil. Prior to the analysis, each material was cleaned by argon-ion etching. All the intermetallic phases and the corresponding pure metals were analyzed. All spectra were normalized to the current of the incident light beam at the moment of data acquisition. Most analysis was based on the platinum $3d_{3/2}$ and $3d_{5/2}$ peaks, since these were present at a very high resolution in the spectra registered for all materials.

The metal disk test-pieces characterized by the above procedure were embedded concentrically, under pressure, in a Teflon rod, to form a rotating-disk electrode. The platinum or intermetallic exposed surface was ground flush with its sheath, using a series of increasingly fine emery papers down to 1200, and then polished with a suspension of alumina (particle size 1 and 0.05 μm) to a mirror finish.

Any reliable comparison of the influence of different electrode materials on a given electrode reaction must take into account the real surface area where the reaction takes place. Accordingly, special care was taken in this study to estimate the active surface area of the electrodes studied. In the absolute absence of a single method that could be applied equally well to all the materials, various methods were employed, according to the specific characteristics of each surface. Even though this approach incurred distinct errors in the areas determined, we are absolutely convinced that it is far better than simply using the electrode geometric areas. Thus, a voltammetric profile was recorded for the polished Pt surface in 0.15 M $HClO_4$, to allow its active area to be calculated from the adsorbed charge of atomic hydrogen [31]. The active area of the PtSb surface was determined by measuring the charge involved in the adsorption of CO *via* Fourier transform infrared spectroscopy (FT-IR) [32]. Active areas of the other intermetallic surfaces were obtained by comparing their degree of roughness with that of the PtSb surface. Roughness was measured by STM.

Electrochemical measurements were made in a two-compartment cell designed hydrodynamically for the RDE, with a reversible hydrogen electrode (RHE) as reference, a platinum wire as counter electrode and 0.15 M $HClO_4$ as electrolyte (Merck, AR). The working electrode, of polished Pt or intermetallic RDE, was used to study the kinetics and mechanism of the HOR. Currents were measured on the Pt or PtM surface of the working electrode during linear potential sweeps from 0 to 0.3 V, at various speeds of rotation from 100 to 3500 rpm, at room temperature. The experiments were carried out with a Pine Instruments Analytical Rotator system coupled to an EG&G-PAR model 283 Potentiostat/Galvanostat, controlled by M270 software. Prior to each experiment, the electrolytic solution was purged with bubbling N_2 (White Martins, 5.0) for 15 min, to remove all traces of O_2, and then saturated with H_2 (AGA, SS) by bubbling for 5 min. Voltammograms were recorded at each speed of rotation and, between each speed, H_2 was bubbled for 1 min to maintain saturation.

Steady state measurements were performed by a chronoamperometric technique. A previously determined pulse potential was applied to the working electrode and the resulting steady-state current recorded after 10 s. During the data acquisition the electrode was rotated at 3500 rpm. A few other rotation speeds were also investigated and no significant difference was observed in the data collected. The electrode potential interval scanned was 0–0.03 V.

3. Results and discussion

3.1. Characterization of ordered intermetallic phases

3.1.1. X-ray diffraction

Fig. 1 displays the X-ray diffractograms obtained for all the investigated materials. All the diffraction profiles were excel-

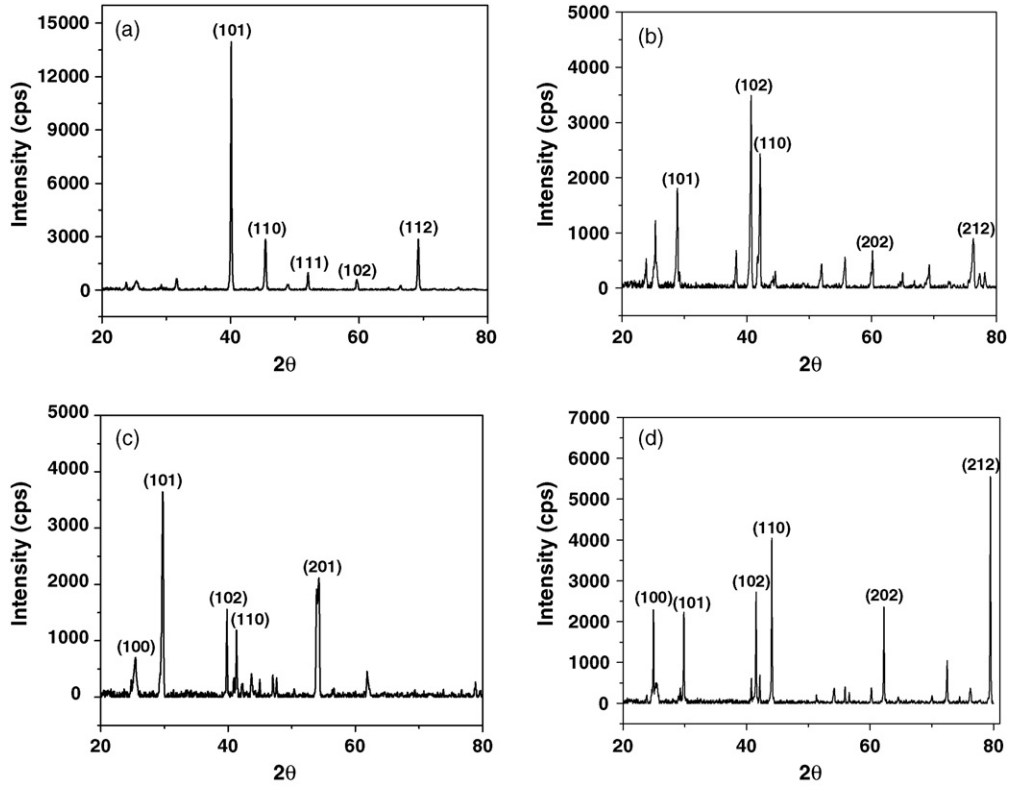

Fig. 1. X-ray diffractograms of the materials: (a) PtMn, (b) PtPb, (c) PtSb and (d) PtSn (Cu cathode, λ = 1.5406 Å).

Table 1
Crystallographic data for the ordered intermetallic phases PtM and polycrystalline Pt

Material	System	Group	Distances (Å)	
			a	*b*
Pt	Cubic	$Fm\bar{3}m$	3.92	3.92
PtMn	Tetragonal	*P*4/*mmm* (123)	4.24	5.48
PtPb	Hexagonal	$P6_3/mmc$ (194)	4.13	5.47
PtSb	Hexagonal	$P6_3/mmc$ (194)	4.10	5.44
PtSn	Hexagonal	$P6_3/mmc$ (194)	2.83	3.67

lent, attesting to the crystallinity of the material. The collected data were compared to the Power Diffraction Files (PCPDFWin, Version 2.4, JCODS-ICDD) and it was confirmed unequivocally that the specimens consisted of the intermetallic phases, with no impurities detected by XRD. Crystallographic parameters for each material are collected in Table 1. The observed changes in the crystallographic parameters from those of the pure starting metals is one of the main features of successful intermetallic phase formation.

3.1.2. X-ray photoelectron spectroscopy

The XPS spectrum obtained for Pt, over the whole binding energy range scanned in this work, is reproduced in Fig. 2. In general, the peaks corresponding to the various inner-shell orbitals were very well-defined. For the purposes of this study, the peaks due to the $3d_{3/2}$ and $3d_{5/2}$ Pt orbitals were chosen for the analysis of the electronic densities of the surface adsorption sites. The high intensity and sharpness of these peaks allow us to investigate any actual changes caused by the formation of intermetallic phases. A representative spectrum recorded in the XPS study is displayed in Fig. 3. In comparison with the pure platinum sample, the following shifts to lower binding energy values were observed for the $3d_{3/2}$ and $3d_{5/2}$ orbitals: PtMn (2 eV), PtPb (2 eV) and PtSb (6 eV). PtSn showed no shift for the Pt orbital peaks; however, in this material, a shift of 10 eV to higher binding energies was seen in the Sn $3d_{3/2}$ orbital peak. It was concluded that in general, as expected, the formation of

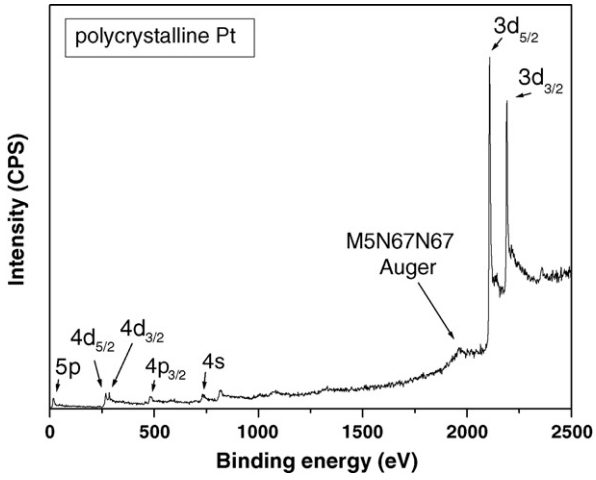

Fig. 2. XPS spectrum obtained from the polycrystalline Pt surface.

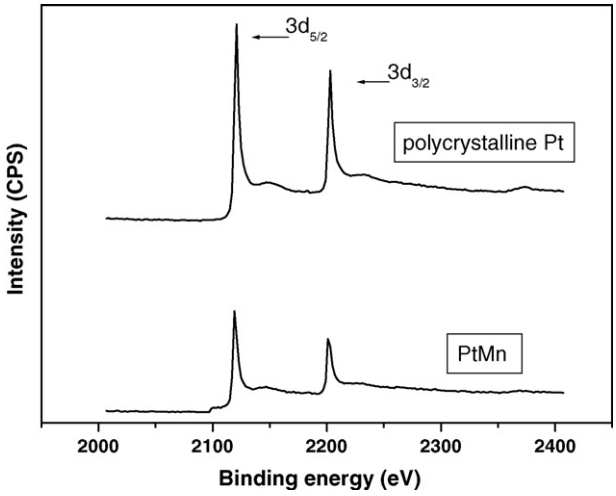

Fig. 3. XPS spectra for Pt $3d_{3/2}$ and $3d_{5/2}$ core-level region obtained from PtMn intermetallic surface.

intermetallic phases led to an effective alteration of the surface atom electron densities that, in its turn, should influence their adsorptive characteristics. This phenomenon has already been noted by other researchers [33–35]. More specifically, Nørskov et al. [34,35] investigated the influence of the d-band center shifts on the strength of adsorptive energy for H_2 and O_2, as the platinum surface sites were alloyed with 3d metals. From their studies it could be seen that the alloying process promotes a significant change in the energy of molecular adsorption that might, in its turn, affect the rate of the overall PEMFC reaction. While it appears that the same phenomenon takes place in the ordered materials investigated in the present study, further analysis of the XPS data regarding electronegativity or the presence of empty orbitals of the component metals in the intermetallic phase [36,37] has proved inconclusive. At any rate, it seems clear that the formation of the intermetallic phases provoked effective changes in the surface site electron densities that would surely influence the adsorption energy of the fuel molecules and, as a consequence, could promote the electrocatalytic activity of these materials towards the hydrogen oxidation reaction.

3.2. Hydrogen oxidation reaction on Pt

The HOR was studied first on a polycrystalline Pt surface, partly to compare its electrocatalytic activity with those of the PtM intermetallic phases and partly to verify experimentally the reliability and precision of the measured RDE hydrodynamic parameters by comparison with published data.

Fig. 4 displays curves of the current generated by the Pt RDE, rotating at 10 different speeds (100–3500 rpm) in dilute perchloric acid saturated with H_2 gas, during linear potential sweeps from 0 to 0.3 V.

Assuming laminar flow, the mass transport rate and, consequently, the limiting diffusional current density can be described mathematically by the Levich equation, as a function of the rotational frequency of the RDE, ω (rpm) [29]:

$$i_d = 0.20nFD^{2/3}\nu^{-1/6}c_0\omega^{1/2} = Bc_0\omega^{1/2} \quad (1)$$

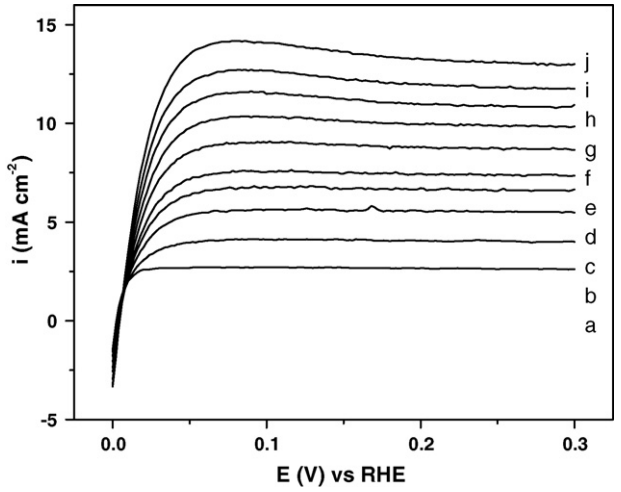

Fig. 4. Linear-sweep voltammograms for Pt RDE in 0.15 M $HClO_4$ solution saturated with H_2 (scan rate 20 mV s^{-1}). Rotation speeds: a = 100 rpm, b = 250 rpm, c = 500 rpm, d = 750 rpm, e = 1000 rpm, f = 1500 rpm, g = 2000 rpm, h = 2500 rpm, i = 3000 rpm and j = 3500 rpm.

where F is the Faraday's constant, D the diffusion coefficient of H_2 in the electrolyte, n the number of electrons in the HOR ($n = 2$), ν the kinematic viscosity of the electrolyte and c_0 the solubility of H_2 in 0.15 M $HClO_4$.

The total current density, in a process controlled equally by activation (charge transfer) and diffusion (mass transport), can be expressed in terms of the kinetic (i_k) and diffusional (i_d) current densities, as follows [29]:

$$\frac{1}{i} = \frac{1}{i_d} + \frac{1}{i_k} = \frac{1}{i_k} + \frac{1}{Bc_0\omega^{-1/2}} \quad (2)$$

Current data obtained at a fixed potential were plotted on a Koutecky–Levich plot (axes i^{-1} versus $\omega^{-1/2}$), as can be seen for 0.2 V in Fig. 5. By applying Eq. (2), straight lines fitted to these data points were used to estimate i_k from their intercepts with the i^{-1} axis and Bc_0 from their slopes. Data for 100 rpm were excluded from the linear regression, owing to the small deviations from calculated values that occur in the limiting diffusional current at low rotational speeds. These deviations arise from the low solubility of H_2 in the electrolyte [3]. The slope of the line in Fig. 5 is 3.61, from which the value of Bc_0 is the reciprocal, 27.7×10^{-2} mA cm^{-2} $rpm^{-1/2}$, while the ordinate intercept is at 0.018 $(mA\,cm^{-2})^{-1}$, yielding a minimum kinetic current density of $i_k = 55$ mA cm^{-2}. This value is around three times the maximum value for the limiting diffusional current density ($i_d \leq 16.4$ mA cm^{-2}), showing that the rate of the HOR at the Pt electrode surface is controlled by mass transport, i.e. by diffusion. Similar i_k values were obtained for the HOR on Pt, in 0.5 M H_2SO_4 electrolyte, by Gasteiger et al. [3]: $i_k \geq 60$ mA cm^{-2}. On the other hand, their values for Bc_0 (5.78×10^{-2} mA cm^{-2} $rpm^{-1/2}$) and i_d ($\leq$3.5 mA cm^{-2}) were not similar to the present values, since these quantities depend on the concentration and type of electrolyte, in this case 0.5 M H_2SO_4 as opposed to 0.15 M $HClO_4$. These results attest to the adequacy of the chosen experimental set-up for reliable measurement of kinetic parameters of the HOR on metal surfaces.

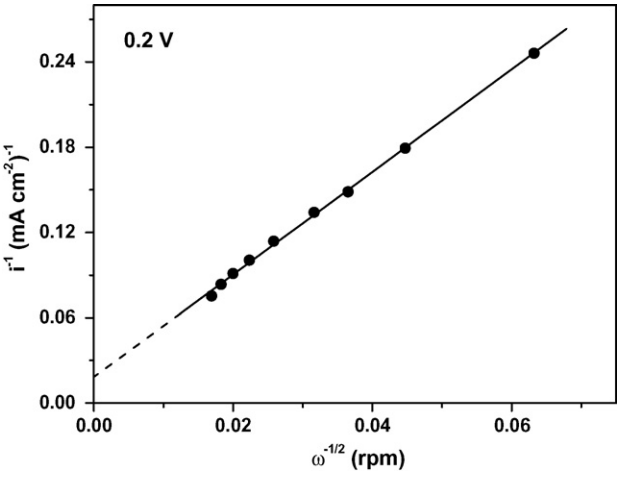

Fig. 5. Koutecky–Levich plot of linear-sweep data for Pt RDE at 0.2 V (see Fig. 4). Data for ω = 100 rpm were excluded from the regression.

Notwithstanding this, there is an inherent lack of precision in i_k determination from Koutecky–Levich plots that leads to doubts about applying them in the evaluation of new electrode materials. In order to overcome this limitation of the technique employed, steady-state experiments were also carried out, as a means of verifying and complementing the RDE results. Thus, steady-state data were used to build up Tafel plots for the HOR on each investigated electrode material.

A Tafel plot is a useful way of obtaining mechanistic and kinetic information for electrode reactions and it is used intensively for the HOR [2,38,39]. Table 2 shows the theoretically predicted mechanistic Tafel information for the HOR in acid medium [38]. On polycrystalline platinum, the most widely accepted mechanism in acid medium is the chemical adsorption step (Tafel) or electrochemical adsorption step (Heyrovsky), followed by the adsorbed hydrogen atom discharge step (Volmer) [1,39], as described in Eqs. (3)–(5):

$$H_2 + 2M \rightarrow 2MH \text{ (Tafel)} \quad (3)$$

$$H_2 + M \rightarrow MH + H^+ + e^- \text{ (Heyrovsky)} \quad (4)$$

$$MH \rightarrow M + H^+ + e^- \text{ (Volmer)} \quad (5)$$

The rates of reactions (3) and (4) can be effectively changed by altering the properties of the electrode surface and the electrolyte. On polycrystalline platinum in a strongly acid medium the Tafel–Volmer mechanism has been proposed, with Tafel as the rate-determining step (rds) [39]. Markovic and co-workers [38] studied the HOR on Pt (1 1 0) in 0.05 M H_2SO_4 at 303 K, and found a Tafel coefficient of 28 mV dec^{-1}. In the present work, a Tafel plot for the HOR on Pt (Fig. 6), corrected for mass

Table 2
Theoretical Tafel parameters and mechanisms for HOR in acid medium at 25 °C

Mechanism	rds	b (mV dec^{-1})[a]
Tafel–Volmer	Tafel	30
Heyrovsky–Volmer	Heyrovsky	118
Tafel–Volmer, Heyrovsk–Volmer	Volmer	59

[a] $b = RT/\beta F$.

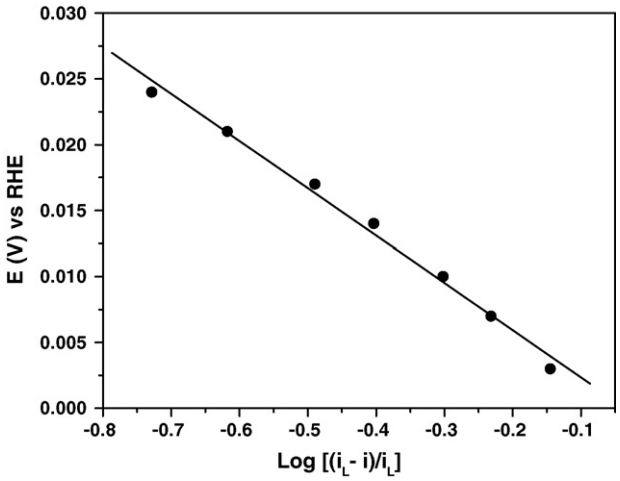

Fig. 6. Mass-transfer corrected Tafel plots for the HOR on Pt in 0.15 M $HClO_4$.

transport influence, produced a value of $b = 36$ mV dec^{-1} in similar experimental conditions. From these results it is reasonable to propose that the HOR takes place on Pt *via* the Tafel–Volmer mechanism with Tafel as rds. It must also be pointed out that the apparent exchange current density (i_0) estimated in the present work (1.08 mA cm^{-2}) was found to be in excellent agreement with the value reported by Markovic et al. (0.98 mA cm^{-2}) for the same reaction in similar conditions.

In conclusion, it has been shown that steady-state experiments can be efficiently used to complement RDE results, in order to obtain reliable data concerning the mechanism and kinetics of the HOR.

Table 3
Kinetic parameters for the HOR on Pt and intermetallic (PtM) electrodes in 0.15 M perchloric acid at room temperature

Material	i_k (mA cm^{-2})	i_d (mA cm^{-2})	Bc_0 mA cm^{-2} rpm$^{-1/2}$
Pt	55	16.4	27.7×10^{-2}
PtMn	15	7.88	13.3×10^{-2}
PtPb	0.93	8.87	15.0×10^{-2}
PtSb	115	4.77	8.00×10^{-2}
PtSn	69	6.29	10.6×10^{-2}

3.3. Oxidation of hydrogen on the intermetallic phases PtM (M = Mn, Pb, Sb and Sn)

The voltammetric curves for RDEs of (a) PtMn, (b) PtPb, (c) PtSb and (d) PtSn in perchloric acid saturated with H_2 gas, obtained during linear sweeps from 0.0 to 0.3 V, at different rotational speeds from 100 to 3500 rpm, are displayed in Fig. 7.

Results from linear regression in Koutecky–Levich plots are shown in Fig. 8, for data recorded at 0.2 V with RDEs of PtSb, PtMn and PtSn and at 0.25 V with PtPb. The values of kinetic parameters of the HOR, measured on the Pt and PtM electrodes in $HClO_4$ solution, are collected in Table 3.

The kinetic current density, i_k is an extremely important electrochemical parameter for evaluating materials as anodes for

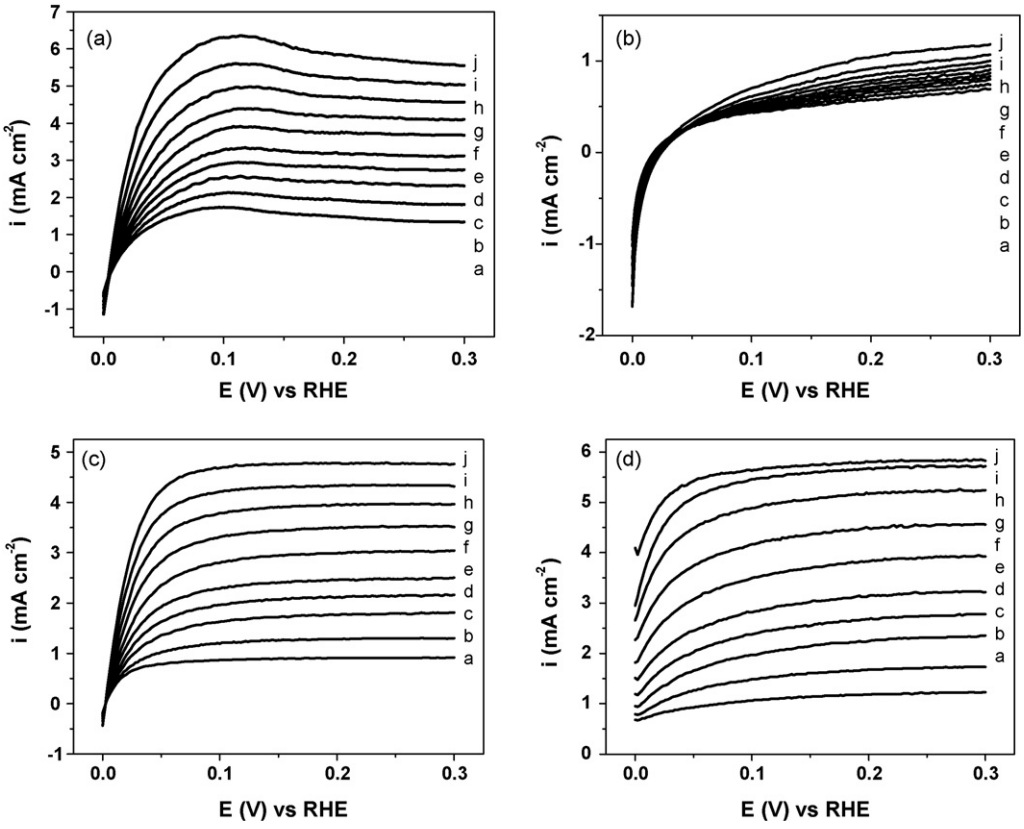

Fig. 7. Linear-sweep voltammograms for RDEs of (a) PtMn, (b) PtPb, (c) PtSb and (d) PtSn in 0.15 M $HClO_4$ solution saturated with H_2 (scan rate 20 mV s^{-1}). Rotation speeds: $a = 100$ rpm, $b = 250$ rpm, $c = 500$ rpm, $d = 750$ rpm, $e = 1000$ rpm, $f = 1500$ rpm, $g = 2000$, $h = 2500$ rpm, $i = 3000$ rpm and $j = 3500$ rpm.

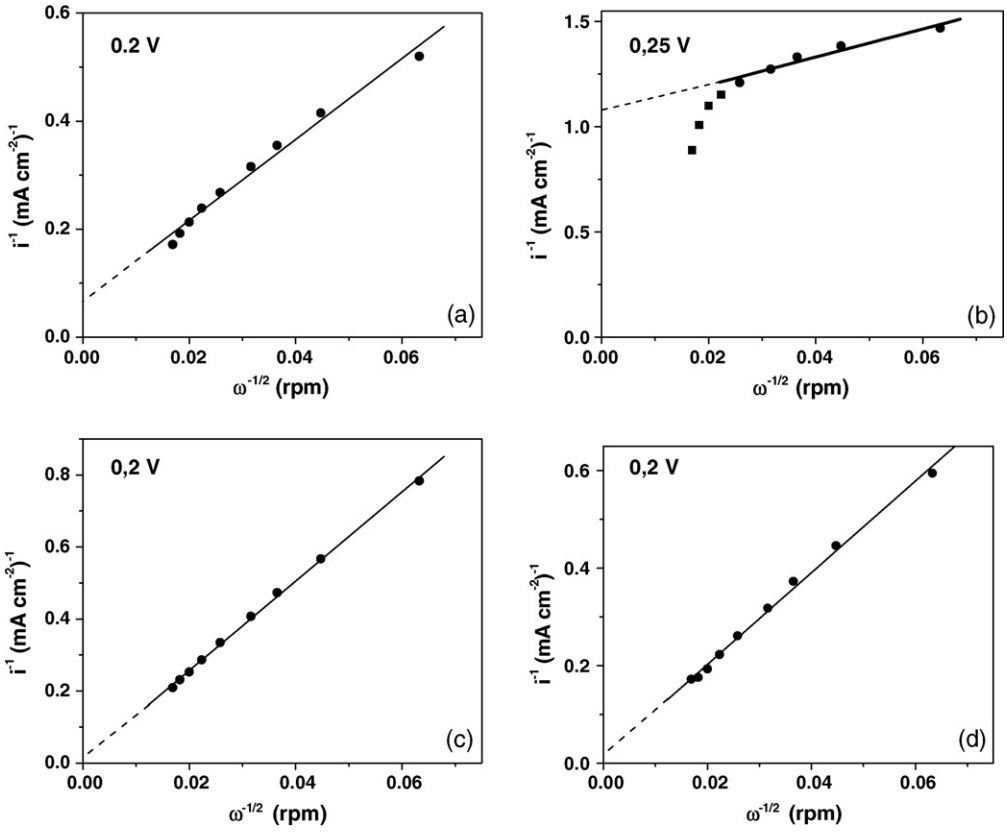

Fig. 8. Koutecky–Levich graph of linear-sweep data (see Fig. 7) for RDEs of (a) PtMn, (b) PtPb, (c) PtSb and (d) PtSn. Data for $\omega = 100$ rpm were excluded from the regression.

hydrogen oxidation, as it is a measure of the rate of charge transfer during oxidation of H_2 at the surface of the anode. In other words, the value of i_k describes the real kinetics of the anode reaction and therefore may be directly related to the electrocatalytic activity of the anode material.

Examination of Table 3 reveals that, except on PtPb, the HOR on the intermetallic anodes was found to be controlled by diffusion. In Fig. 7(b), the voltammetric profile for PtPb, it can be seen in the set of very similar curves that the HOR showed very little activity on this electrode, even at higher speeds of rotation. The i_k and i_d data in Table 3 suggest that the PtPb anode was the only one to exhibit a reaction controlled by charge transfer (ie. activation), consistently with its low and ω-independent activity. The extremely low value of i_k may be due to some process deactivating the surface, or the inherent ineffectiveness of this electrode surface towards the HOR.

Comparing the data for Pt in Table 3 with those for the intermetallic anodes, the value of i_k for the HOR on PtMn is lower than on Pt, implying that PtMn has poorer electrocatalytic activity than Pt with respect to the HOR. In contrast, the intermetallic phases PtSb and PtSn exhibit kinetic current densities around 2.1 and 1.3 times that for Pt, respectively. Such enhanced performance is encouraging, especially when the relatively lower amount of Pt in these materials is recalled.

Fig. 9 shows the Tafel plots obtained for the HOR at the ordered intermetallic electrode surfaces. The corresponding Tafel parameters and the proposed mechanisms are assembled in Table 4. For purposes of comparison, the same information obtained for Pt is also presented. In Table 4, it is observed that PtSb and PtSn produced b values close to 59 mV dec^{-1}, pointing to the occurrence of the reaction *via* a fast chemical (Tafel) or electrochemical (Heyrovsky) adsorption step, followed by a slow adsorbed hydrogen atom discharge step (Volmer). The PtMn b value, in contrast, is 176 mV dec^{-1}, suggesting the occurrence of a Heyrovsky–Volmer mechanism with Heyrovsky as rds. However, this calculated value for b is appreciably larger than the theoretically predicted value (118 mV dec^{-1}; see Table 2), pointing to the influence of some other process taking place alongside the HOR. Additionally, the anomalous b value found for the HOR on PtPb does not allow any mechanistic consideration to be made. As a general rule, it was found that the adsorption steps were greatly enhanced in the HOR on the intermetallic surfaces, since those steps were no longer found to

Table 4
Kinetic and mechanistic parameters obtained for the HOR on Pt and ordered intermetallic phases PtM in 0.15 M $HClO_4$ at room temperature

Material	b (mV dec^{-1})	i_0 (mA cm^{-2})	Mechanism	rds
Pt	36	1.08	Tafel–Volmer	Tafel
PtMn	176	1.19	Heyrovsky–Volmer	Heyrovsky
PtPb	385	1.07	–	–
PtSb	55	2.35	Tafel/Heyrovsky–Volmer	Volmer
PtSn	59	1.53	Tafel/Heyrovsky–Volmer	Volmer

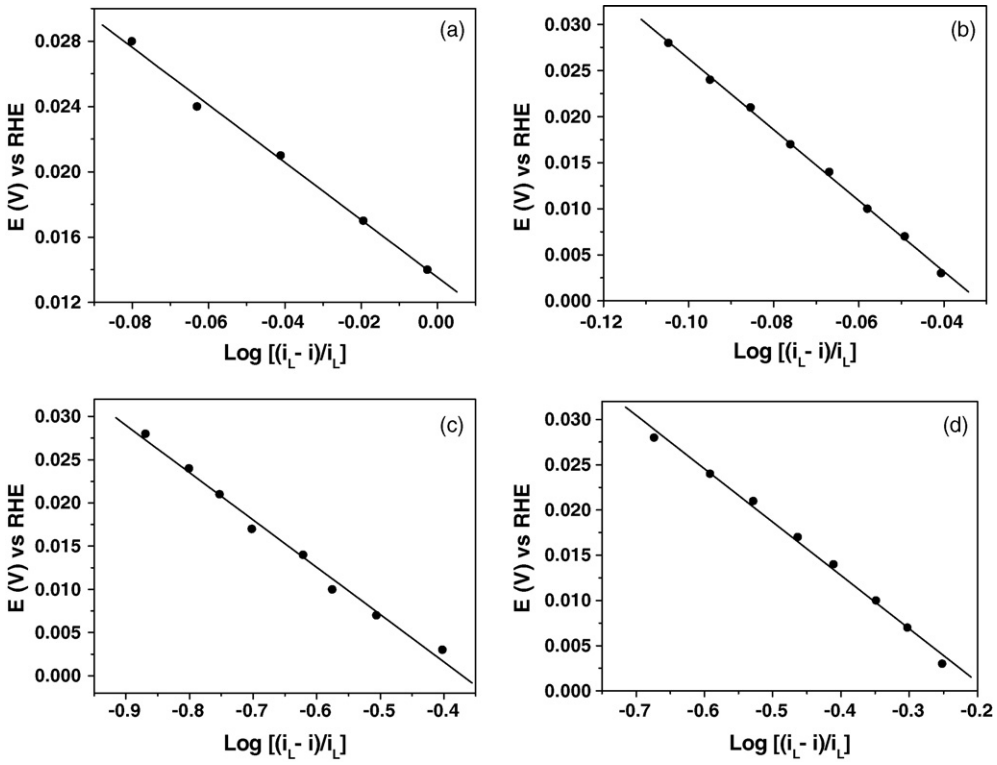

Fig. 9. Mass-transfer corrected Tafel plots for the HOR on: (a) PtMn, (b) PtPb, (c) PtSb and (d) PtSn in 0.15 M $HClO_4$.

determine the rate of the overall reaction. The results unequivocally point to the enhancement of the adsorptive characteristic of the intermetallic surfaces, compared to Pt.

From Table 4 it is observed that PtSb and PtSn produced i_0 values, respectively, 2.2 and 1.4 times higher than the Pt value, indicating a better electrocatalytic activity of the intermetallic surfaces towards the HOR and also confirming the kinetic evaluation from RDE data, in comparison with Pt. On the other hand, PtMn performed similarly to Pt in the HOR, according to Tafel plot analysis, while the same material produced a quite lower i_k value than Pt in the RDE experiments. As previously mentioned, the low performance of the PtPb intermetallic material towards the HOR does not allow any mechanistic or kinetic consideration to be made.

The performance of the intermetallic phases in the HOR might be influenced by two properties of the anode surface: the disposition of the active sites on the surface (both Pt and M sites) and alterations of the surface electron density pattern from that of pure Pt. The first property was investigated by analyzing the powder XRD patterns recorded during characterization of the materials. Examining the distances between Pt–Pt, Pt–M and M–M sites, it was noted that they have no influence on the HOR at these surfaces, as there is no obvious correlation between the interatomic distances and i_k or i_0 values for Pt and the intermetallic phases shown in Tables 3 and 4. This is consistent with the relatively small size of the H_2 molecule, which should make the distance between metallic surface sites of secondary importance in its oxidation. Conversely, changes in the electron density at the surface sites must be highly relevant to the electrocatalytic activity of the intermetallic phases; the formation of these phases leads to a distribution of electrons on the surface quite different from that of the pure elements, which certainly will have some effect on the activity of the surface when catalyzing the HOR.

The problem of interpreting the shifts in binding energies at the surface of an intermetallic compound in terms of its surface electron-density map is not a trivial one, and researchers have so far been unable to elucidate the relation between XPS results and electron density [40]. It is worth noting that Sn and Sb have similar electronegativities relative to Pt and thus both metals could induce a significant change in the electron density at the Pt sites. More detailed experimental and theoretical study is in progress, to try and clarify the relationship between the binding-energy band shifts detected by XPS and the surface electron-density pattern, so that eventually the kinetic and mechanistic data for the HOR on the intermetallic anodes may be more readily interpreted. However, it was clearly demonstrated that the electron redistribution mainly influenced the adsorption characteristic of the hydrogen molecule on the intermetallic surface that, in its turn, enhanced the adsorption steps of the HOR mechanism.

Furthermore, it can already be reported that the evaluation of ordered intermetallic phases proved a good strategy for the development of novel electrocatalysts for the HOR, since it was possible, by varying the transition metal constituents, to vary the surface structure and electron distribution in a controlled way. Moreover, and no less importantly, it should be noted that these anode materials contain 50% less Pt than the reference catalysts (pure Pt) and are thus appreciably less expensive.

4. Conclusion

Kinetic studies have shown that, when used to catalyze the HOR in acid medium, PtSb and PtSn ordered intermetallic phases produced i_k values, respectively, 2.1 and 1.3 times higher than a Pt electrode and i_0 values 2.2 and 1.4 times higher than Pt in the same experimental conditions. The better performance of these materials was attributed to alteration of the electron density of the surface adsorption sites, which markedly improved the adsorption of hydrogen molecules on the surface. As a consequence of this effect, the mechanism proposed for the HOR on these materials involves Tafel/Heyrovsky–Volmer steps, with Volmer as rds.

Acknowledgments

The authors acknowledge the grants awarded by the following Brazilian authorities: Fundaçao de Amparo à Pesquisa do Estado de São Paulo (FAPESP), Conselho Nacional de Desenvolvimento Científico e Tecnológico (CNPq) and the Ministério da Ciência e Tecnologia (MCT-PROCaC), without which this research would not have been completed. Costs of publication of this article were partly covered by the UNESP Pro-Reitoria de Pesquisa (PROPe-PICR), São Paulo, Brazil.

References

[1] L. Carrette, K.A. Friedrich, U. Stimming, Fuel cells—fundamentals and applications, Fuel Cells 1 (2001) 5–39.
[2] P.M. Quaiano, M.R.G. De Chialvo, A.C. Chialvo, Phys. Chem. Chem. Phys. 6 (2004) 4450–4455.
[3] H.A. Gasteiger, N.M. Markovic, P.N. Ross, J. Phy. Chem. 99 (1995) 8290–8301.
[4] H.A. Gasteiger, N.M. Markovic, P.N. Ross, J. Phys. Chem. 99 (1995) 8945–8949.
[5] H.A. Gasteiger, N.M. Markovic, P.N. Ross, J. Phys. Chem. 99 (1994) 16757–16767.
[6] N.M. Markovic, A. Widelov, P.N. Ross, O.R. Monteiro, I.G. Brown, Catal. Lett. 43 (1997) 161–166.
[7] W. Vielstich, Fuel Cells; Modern Processes for the Electrochemical Production of Energy, Wiley–Interscience, New York, 1970, pp. 501.
[8] E.V. Spinacé, A.O. Neto, E.G. Franco, M. Linardi, E.R. Gonzalez, Química. Nova 27 (2004) 648–654.
[9] D. Pletcher, V.J. Solis, J. Electroanal. Chem. 131 (1982) 309–323.
[10] J. Clavilier, S.G. Sun, J. Electroanal. Chem. 199 (1986) 471–480.
[11] S.C. Chang, Y.H. Ho, M.J. Weaver, Surf. Sci. 265 (1992) 81–94.
[12] E. Herrero, M.J. Llorca, J.M. Feliu, A. Aldaz, J. Electroanal. Chem. 383 (1994) 145–154.
[13] V. Climent, E. Herrero, J.M. Feliu, Electrochim. Acta 44 (1998) 1403–1414.
[14] M. Shibata, S. Motoo, J. Electroanal. Chem. 188 (1985) 111–120.
[15] L.R. Dollard, R.W. Evanse, G.A. Attard, J. Electroanal. Chem. 345 (1993) 205–221.
[16] M.J. Llorca, E. Herrero, J.M. Feliu, A. Aldaz, J. Electroanal. Chem. 373 (1994) 217–225.
[17] E. Leiva, T. Iwasita, E. Herrero, J.M. Feliu, Langmuir 13 (1997) 6287–6293.
[18] G.Y. Jung, H.S. Park, C.K. Rhee, J. Electroanal. Chem. 453 (1998) 243–247.
[19] W.F. Lin, M.S. Zei, M. Eiswirth, G. Ertl, T. Iwasita, W. Vielstich, J. Phys. Chem. B 103 (1999) 6968–6977.
[20] T.J. Schmidt, R.J. Behm, B.N. Grgur, N.M. Markovic, P.N. Ross, Langmuir 16 (2000) 8159–8166.
[21] S.P.E. Smith, K.F. Ben-Dor, H.D. Abruna, Langmuir 15 (1999) 7325–7332.
[22] T.J. Schmidt, V.R. Stamenkovic, C.A. Lucas, N.M. Markovic, P.N. Ross, Phys. Chem. Chem. Phys. 3 (2001) 3879–3890.
[23] G. Wittstock, A. Strubing, R. Szargan, G.J. Werner, J. Electroanal. Chem. 444 (1998) 61–73.
[24] U. Hamm, D. Kramer, R.S. Zhai, D.M. Kolb, Electrochim. Acta 43 (1998) 2969–2978.
[25] S.P.E. Smith, H.D.J. Abruna, J. Phys. Chem. B 102 (1998) 3506–3511.
[26] S.P.E. Smith, H.D.J. Abruna, J. Electroanal. Chem. 467 (1999) 43–49.
[27] E. Casado-Rivera, Z. Gal, A.C.D. Angelo, C. Lind, F.J. Disalvo, H.D. Abruna, Chemphyschem 4 (2003) 193–199.
[28] E. Casado-Rivera, D.J. Volpe, L. Alden, C. Lind, C. Downie, T. Vazquez-Alvarez, A.C.D. Angelo, F.J. Disalvo, H.D. Abruna, J. Am. Chem. Soc. 126 (2004) 4043–4049.
[29] E. Gileadi, Electrode Kinetics for Chemists, Chemical Engineers and Material Scientists, VCH Publishers, New York, 1993, pp. 82–91.
[30] W.G. Moffatt, Binary Phase Diagrams Handbook, General Electric Co., 1976.
[31] M. Breiter, H. Kammermaier, C.A. Knorr, Zeitschrift fuer Elektrochemie und Angewandte Physikalische Chemie 60 (1956) 37–47.
[32] J.P.I. de Souza, S.L. Queiroz, K. Bergamaski, E.R. Gonzalez, F.C. Nart, J. Phys. Chem. B 106 (2002) 9825–9830.
[33] J. Zhang, M.B. Vukmirovic, Y. Xu, M. Mavrikakis, R.R. Adzic, Angew. Chem. (International ed. In English) 44 (2005) 2132–2135.
[34] J.R. Kitchin, J.K. Nørskov, M.A. Barteau, J.G. Chen, J. Chem. Phys. 120 (2004) 10240–10246.
[35] V. Pallassana, M. Neurock, L.B. Hansen, J.K. Nørskov, J. Chem. Phys. 112 (2000) 5435–5439.
[36] J.A. Rodriguez, R.A. Campbell, D.W. Goodman, J. Phys. Chem. 95 (1991) 5716–5719.
[37] J.A. Rodriguez, R.A. Campbell, D.W. Goodman, J. Vacuum Sci. Technol. A: Vacuum Surf. Films 9 (1991) 1698–1702.
[38] N.M. Markovic, B.N. Grgur, P.N. Ross, J. Phys. Chem. B 101 (1997) 5405–5413.
[39] R.M.Q. Mello, E.A. Ticianelli, Electrochim. Acta 42 (1997) 1031–1039.
[40] P.M.Th.M. van Attekum, J.M. Trooster, J. Phys F: Metal. Phys. 9 (1979) 2287–2300.